Low-frequency dispersion characteristics of the multi-layered coaxial cable

Nordebo, Sven; Nilsson, Börje; Biro, Thomas; Cinar, Gökhan; Gustafsson, Mats; Gustafsson, Stefan; Karlsson, Anders; Sjöberg, Mats

2011

CODEN:LUTEDX/(TEAT-7212)/1-20/(2011)

Low-frequency dispersion characteristics of the multi-layered coaxial cable

Sven Nordebo, Börje Nilsson, Thomas Biro, Gökhan Cinar, Mats Gustafsson, Stefan Gustafsson, Anders Karlsson, and Mats Sjöberg

Electromagnetic Theory
Department of Electrical and Information Technology
Lund University
Sweden

Sven Nordebo, Börje Nilsson, Stefan Gustafsson
{sven.nordebo,borje.nilsson,stefan.h.gustafsson}@lnu.se

School of Computer Science, Physics and Mathematics
Linnaeus University
SE-351 95 Växjö
Sweden

Thomas Biro
thomas.biro@jth.hj.se

School of Engineering
Jönköping University
SE-551 11 Jönköping
Sweden

Gökhan Cinar
gokhan_cinar@yahoo.com

Electronics Engineering Department
Gebze Institute of Technology
414 00 Gebze, Kocaeli
Turkey

Mats Gustafsson, Anders Karlsson
{mats.gustafsson,anders.karlsson}@eit.lth.se

Department of Electrical and Information Technology
Electromagnetic Theory
Lund University
P.O. Box 118
SE-221 00 Lund
Sweden

Mats Sjöberg
mats.l.sjoberg@se.abb.com

ABB AB
SE-371 23 Karlskrona
Sweden

Editor: Gerhard Kristensson

Abstract

This paper provides an exact asymptotic analysis regarding the low-frequency dispersion characteristics of the multi-layered coaxial cable. A layer-recursive description of the dispersion relation is derived and analyzed. It is shown that if there is one isolating layer and a perfectly conducting outer shield, the classical Weierstrass preparation theorem can be used to prove that the low-frequency behavior of the propagation constant is governed by a square root of the complex frequency, and an exact analytical expression for the dominating term of the asymptotic expansion is derived. It is furthermore shown that the same asymptotic expansion is valid to its lowest order even if the outer shield has finite conductivity and there is an infinite exterior region with finite non-zero conductivity. The proofs are based on asymptotic analysis, and illustrated with numerical examples. As a practical application of the theory, a High-Voltage Direct Current (HVDC) power cable is analyzed and a numerical solution to the dispersion relation is validated by comparisons with the asymptotic analysis. The comparison reveals that the low-frequency dispersion characteristics of the power cable is very complicated and a first order asymptotic approximation is valid only at extremely low frequencies (below 1 Hz). Hence, for practical modeling purposes such as with fault localization etc., an accurate numerical solution to the dispersion relation is of great value.

1 Introduction

The topic of this paper is to perform an exact asymptotic analysis regarding the low-frequency dispersion characteristics of the multi-layered coaxial cable. Except for the general physical insight and development of mathematical methods, this study is motivated by the need to understand the precise behavior of the low-frequency wave propagation characteristics of High-Voltage Direct Current (HVDC) power cables. It is anticipated that accurate electromagnetic models will potentially be very useful for future fault localization and diagnosis systems regarding the surveillance of very long HVDC power cables [1, 2, 8, 10, 14, 16, 17, 19]. To this end, a low-frequency approximation of the propagation constant can potentially be very useful as part of an efficient numerical method to solve the electromagnetic problem. On the other hand, a numerical algorithm to solve the electromagnetic problem can also be validated by comparisons with the correct asymptotics at low frequencies.

The HVDC power cables constitute good examples of a multi-layered coaxial cable. The wave propagation characteristics of transmission lines and power cables have been studied over many years, see *e.g.*, [4, 5, 9, 13, 18]. Recent studies have been devoted to measurements and modeling regarding the semiconducting layers of a power cable and its effect on wave propagation characteristics [1, 2, 16]. It has been shown, *e.g.*, that the semiconducting layer contributes significantly to the attenuation for frequencies above 5-10 MHz [16]. However, in applications regarding fault localization and surveillance of very long (10 km or more) HVDC power cables, the relevant frequency range is rather in the low-frequency regime of about 0-100 kHz, see [10].

It is observed that many of the classical results such as in [1, 4] are based on approximations and restrictions rather than general electromagnetic modeling and accurate numerical solutions of the related dispersion relation. Hence, in [1, 4], low-frequency approximations are incorporated where the longitudinal wave number is partly neglected and the exact dispersion relation is avoided. These approximations may not be accurate enough if a precise evaluation is required with respect to the properties of a multi-layered coaxial power cable.

A layer-recursive description of the dispersion relation for the axial-symmetric Transversal Magnetic TM_{0n} modes is derived and analyzed in this paper. It will be shown that when the cable has at least one isolating layer, the propagation constant of the dominating TM_{01} mode tends to zero as the frequency tends to zero, but it is not an analytic function in a neighborhood of the zero frequency. By employing the classical Weierstrass preparation theorem (Theorem 7.5.1 in [6]) it is shown that if there is one isolating layer and a perfectly conducting outer shield, the low-frequency behavior of the propagation constant γ of the dominating mode is governed by a square root of the complex frequency $\gamma \sim A\sqrt{\mathrm{i}\omega/\mathrm{c}_0}$, and an exact analytical expression for the dominating term of the asymptotic expansion is derived. It is furthermore shown that the same asymptotic expansion is valid to its lowest order even if the outer shield has finite conductivity and there is an infinite exterior region with finite non-zero conductivity. The proofs are based on asymptotic analysis, and illustrated with numerical examples.

A HVDC power cable is analyzed and a numerical solution to the dispersion relation is validated by comparisons with the asymptotic analysis. In this example case, it is concluded that the low-frequency behavior of the propagation constant is rather complicated and the first order asymptotic approximation is not accurate enough to model the cable response over the relevant frequency range $0-100\,\mathrm{kHz}$. An accurate numerical solution to the dispersion relation is hence very useful, see [10].

The rest of the paper is organized as follows: In section 2 is given the basic electromagnetic model and in section 3 the asymptotic analysis. In section 4 is given the numerical examples and in section 5 the summary and conclusions.

2 The electromagnetic model

2.1 Basic definitions and boundary conditions

Let μ_0, ε_0, η_0 and c_0 denote the permeability, the permittivity, the wave impedance and the speed of light in free space, respectively, and where $\eta_0 = \sqrt{\mu_0/\varepsilon_0}$ and $\mathrm{c}_0 = 1/\sqrt{\mu_0\varepsilon_0}$. The wave number of free space is given by $k = \omega/\mathrm{c}_0$ where $\omega = 2\pi f$ is the angular frequency and f the frequency. It follows that $\omega\mu_0 = k\eta_0$ and $\omega\varepsilon_0 = k/\eta_0$. The cylindrical coordinates are denoted by (ρ, ϕ, z), the corresponding unit vectors $(\hat{\boldsymbol{\rho}}, \hat{\boldsymbol{\phi}}, \hat{\boldsymbol{z}})$ and the transversal coordinate vector $\boldsymbol{\rho} = \rho\hat{\boldsymbol{\rho}}$. The time convention is defined by the factor $\mathrm{e}^{\mathrm{i}\omega t}$.

Consider the eigenvalue problem based on Maxwell's equations for a multi-layered circularly symmetrical coaxial cable. The wave propagation along the z-direction

of the coaxial cable is given by the exponential factor $\mathrm{e}^{-\gamma z}$ where γ is the propagation constant corresponding to a particular mode [7, 15]. With the electric and magnetic fields denoted by $\boldsymbol{E} = \boldsymbol{E}(\boldsymbol{\rho}, \gamma)\mathrm{e}^{-\gamma z}$ and $\boldsymbol{H} = \boldsymbol{H}(\boldsymbol{\rho}, \gamma)\mathrm{e}^{-\gamma z}$, respectively, the eigenvalue problem to be solved is given by

$$\left\{\nabla_{\mathrm{t}}^2 + k^2\epsilon + \gamma^2\right\} \left\{ \begin{array}{c} \boldsymbol{E}(\boldsymbol{\rho}, \gamma) \\ \boldsymbol{H}(\boldsymbol{\rho}, \gamma) \end{array} \right\} = \left\{ \begin{array}{c} \mathbf{0} \\ \mathbf{0} \end{array} \right\}, \tag{2.1}$$

together with the appropriate boundary conditions, and where ∇_{t}^2 is the transversal part of the Laplace operator and γ^2 the eigenvalue [7, 15]. It should be noted that the eigenvalue problem (2.1) in general has a continuous spectrum if an exterior infinite domain is included. This complication is also manifested by the presence of a branch-cut in the complex γ-plane related to the dispersion function which will be derived below.

Consider the multi-layered circularly symmetrical coaxial cable as depicted in Figure 1. Here, there are $N+1$ material boundaries with radius ρ_i for $i = 0, 1, \ldots, N$ defining an inner region for $0 \leq \rho \leq \rho_0$ with permittivity ϵ_0, N intermediate layers for $\rho_{i-1} \leq \rho \leq \rho_i$ with permittivity ϵ_i for $i = 1, \ldots, N$ and an outer region for $\rho \geq \rho_N$ with permittivity ϵ_{N+1}.

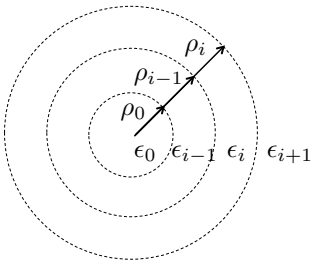

Figure 1: The multi-layered circularly symmetrical coaxial cable with geometrical and material definitions.

The complex valued permittivity in each of the $N + 2$ regions are defined by

$$\epsilon_i = \epsilon_{\mathrm{r}i} - \mathrm{i}\sigma_i\eta_0/k, \;\; i = 0, 1, \ldots, N + 1, \tag{2.2}$$

where $\epsilon_{\mathrm{r}i}$ is the real, relative permittivity and σ_i the conductivity of the material. Further, let

$$\kappa_i = \sqrt{k^2\epsilon_i + \gamma^2}, \;\; i = 0, 1, \ldots, N + 1, \tag{2.3}$$

be the corresponding radial wave number for material region i where the square root[1] is chosen such that $\mathrm{Im}\{\kappa_i\} \leq 0$, see also [3, 10].

The present study is concerned with the Transversal Magnetic (TM) modes of order $m = 0$ denoted TM_{0n}, as the Transversal Electric (TE) modes of order $m = 0$,

[1] To make the square root unique, its phase angle is chosen as $-\pi < \arg\kappa_i \leq 0$.

TE_{0n}, and all the higher order modes[2] with $m \neq 0$ will essentially be cut-off in the low-frequency regime. The electric and magnetic field components are given by an expansion in cylindrical vector waves as defined in *e.g.*, [10], see also [3, 7, 15]. Here, the E_z and H_ϕ field components of the TM_{0n} modes are expressed in each layer by

$$E_z = \frac{1}{2\pi \mathrm{i}} \frac{\kappa}{k} \left[a\psi_0^{(1)}(\kappa\rho) + b\psi_0^{(2)}(\kappa\rho) \right] \mathrm{e}^{-\gamma z}, \tag{2.4}$$

$$H_\phi = \frac{1}{2\pi\eta_0} \epsilon \left[a\psi_1^{(1)}(\kappa\rho) + b\psi_1^{(2)}(\kappa\rho) \right] \mathrm{e}^{-\gamma z}, \tag{2.5}$$

where a and b are complex valued expansion coefficients, and $\psi_m^{(j)}(\cdot)$ a Bessel function or a Hankel function of the first kind ($j = 1$) and the second kind ($j = 2$), and order $m = 0, 1$. Note that the expansion coefficients a and b have the same dimension as the electric field (V/m).

For the intersection between two materials with finite conductivity[3] the appropriate boundary conditions are given by the continuity of the tangential electric and magnetic fields [7]. For the TM_{0n} modes these boundary conditions can be formulated using (2.4) and (2.5) as follows. Let a_0, a_i and b_i for $i = 1, \ldots, N$ and b_{N+1} denote the expansion coefficients corresponding to the $N + 2$ regions defined above. The boundary conditions related to the first boundary at radius ρ_0 are given by

$$\begin{cases} -a_0\kappa_0 \mathrm{J}_0(\kappa_0\rho_0) + a_1\kappa_1 \mathrm{H}_0^{(1)}(\kappa_1\rho_0) + b_1\kappa_1 \mathrm{H}_0^{(2)}(\kappa_1\rho_0) = 0, \\ -a_0\kappa_0 \dfrac{k\epsilon_0}{\kappa_0} \mathrm{J}_1(\kappa_0\rho_0) + a_1 k\epsilon_1 \mathrm{H}_1^{(1)}(\kappa_1\rho_0) + b_1 k\epsilon_1 \mathrm{H}_1^{(2)}(\kappa_1\rho_0) = 0, \end{cases} \tag{2.6}$$

where $\mathrm{J}_m(\cdot)$ denotes the Bessel function of the first kind and $\mathrm{H}_m^{(1)}(\cdot)$ and $\mathrm{H}_m^{(2)}(\cdot)$ the Hankel functions of the first and second kind, respectively, see [12]. Note that $a_0\kappa_0$ together with a_1 and b_1 are regarded to be the unknown coefficients in (2.6). The boundary conditions related to the boundary at radius ρ_{i-1} are similarly given by

$$\begin{cases} -a_{i-1}\kappa_{i-1} \mathrm{H}_0^{(1)}(\kappa_{i-1}\rho_{i-1}) - b_{i-1}\kappa_{i-1} \mathrm{H}_0^{(2)}(\kappa_{i-1}\rho_{i-1}) \\ \qquad + a_i\kappa_i \mathrm{H}_0^{(1)}(\kappa_i\rho_{i-1}) + b_i\kappa_i \mathrm{H}_0^{(2)}(\kappa_i\rho_{i-1}) = 0, \\ -a_{i-1} k\epsilon_{i-1} \mathrm{H}_1^{(1)}(\kappa_{i-1}\rho_{i-1}) - b_{i-1} k\epsilon_{i-1} \mathrm{H}_1^{(2)}(\kappa_{i-1}\rho_{i-1}) \\ \qquad + a_i k\epsilon_i \mathrm{H}_1^{(1)}(\kappa_i\rho_{i-1}) + b_i k\epsilon_i \mathrm{H}_1^{(2)}(\kappa_i\rho_{i-1}) = 0, \end{cases} \tag{2.7}$$

where $i = 2, \ldots, N$. The boundary conditions related to the last boundary at radius ρ_N are finally given by

$$\begin{cases} -a_N\kappa_N \mathrm{H}_0^{(1)}(\kappa_N\rho_N) - b_N\kappa_N \mathrm{H}_0^{(2)}(\kappa_N\rho_N) \\ \qquad + b_{N+1}\kappa_{N+1} \mathrm{H}_0^{(2)}(\kappa_{N+1}\rho_N) = 0, \\ -a_N k\epsilon_N \mathrm{H}_1^{(1)}(\kappa_N\rho_N) - b_N k\epsilon_N \mathrm{H}_1^{(2)}(\kappa_N\rho_N) \\ \qquad + b_{N+1} k\epsilon_{N+1} \mathrm{H}_1^{(2)}(\kappa_{N+1}\rho_N) = 0. \end{cases} \tag{2.8}$$

[2]Note that the TE and TM field components are generally coupled via the boundary conditions, but are always decoupled for the axial symmetric TM_{0n} and TE_{0n} modes.

[3]It is assumed that at least one of the layers have non-zero conductivity so that there are no surface currents.

Note that the inner region is represented solely by the Bessel function $\mathrm{J}_m(\kappa_0\rho)$ (regular wave) in (2.6) and the outer region is represented solely by the Hankel function $\mathrm{H}_m^{(2)}(\kappa_{N+1}\rho)$ (outgoing wave) in (2.8), see also [3, 7, 10, 15].

The row scaling of the boundary conditions in (2.6) through (2.8) using the free space wave number k as well as the definition of the coefficient $a_0\kappa_0$ in (2.6) has been chosen in order to obtain the desired analytical properties of the dispersion function in the subsequent asymptotic analysis. Hence, let the unknown coefficients be $a_0\kappa_0$, together with the coefficients a_i and b_i for $i = 1, \ldots, N$, and b_{N+1}. The boundary conditions in (2.6) through (2.8) are then assembled into a square $(2N+2)\times(2N+2)$ matrix $\mathbf{A}(\gamma^2, k)$, and the corresponding dispersion relation is given by

$$h_{N+1}(\gamma^2, k) = \det \mathbf{A}(\gamma^2, k) = 0, \tag{2.9}$$

which is the condition for the existence of a mode [7, 15].

2.2 The layer-recursive dispersion relation

A layer-recursive representation of the dispersion function $h_{N+1}(\gamma^2, k) = \det \mathbf{A}(\gamma^2, k)$ defined in (2.9) is obtained as follows.

Define the following auxiliary functions based on certain combinations of the Hankel functions

$$\begin{aligned}
a_i(\kappa_i) &= \mathrm{H}_1^{(1)}(\kappa_i\rho_{i-1})\mathrm{H}_0^{(2)}(\kappa_i\rho_i) - \mathrm{H}_1^{(2)}(\kappa_i\rho_{i-1})\mathrm{H}_0^{(1)}(\kappa_i\rho_i),\\
b_i(\kappa_i) &= \mathrm{H}_0^{(2)}(\kappa_i\rho_{i-1})\mathrm{H}_0^{(1)}(\kappa_i\rho_i) - \mathrm{H}_0^{(1)}(\kappa_i\rho_{i-1})\mathrm{H}_0^{(2)}(\kappa_i\rho_i),\\
c_i(\kappa_i) &= \mathrm{H}_1^{(1)}(\kappa_i\rho_{i-1})\mathrm{H}_1^{(2)}(\kappa_i\rho_i) - \mathrm{H}_1^{(2)}(\kappa_i\rho_{i-1})\mathrm{H}_1^{(1)}(\kappa_i\rho_i),\\
d_i(\kappa_i) &= \mathrm{H}_0^{(2)}(\kappa_i\rho_{i-1})\mathrm{H}_1^{(1)}(\kappa_i\rho_i) - \mathrm{H}_0^{(1)}(\kappa_i\rho_{i-1})\mathrm{H}_1^{(2)}(\kappa_i\rho_i),
\end{aligned} \tag{2.10}$$

where $i \geq 1$.

Based on the boundary conditions (2.6) through (2.8), the following determinants are now defined. The zero-order determinants are given by

$$\begin{cases}
f_0(\gamma^2, k) = -\mathrm{J}_0(\kappa_0\rho_0),\\
g_0(\gamma^2, k) = -\dfrac{k\epsilon_0}{\kappa_0}\mathrm{J}_1(\kappa_0\rho_0).
\end{cases} \tag{2.11}$$

The first order determinants are given by

$$f_1(\gamma^2, k) = \begin{vmatrix}
-\mathrm{J}_0(\kappa_0\rho_0) & \kappa_1\mathrm{H}_0^{(1)}(\kappa_1\rho_0) & \kappa_1\mathrm{H}_0^{(2)}(\kappa_1\rho_0)\\
-\dfrac{k\epsilon_0}{\kappa_0}\mathrm{J}_1(\kappa_0\rho_0) & k\epsilon_1\mathrm{H}_1^{(1)}(\kappa_1\rho_0) & k\epsilon_1\mathrm{H}_1^{(2)}(\kappa_1\rho_0)\\
0 & -\kappa_1\mathrm{H}_0^{(1)}(\kappa_1\rho_1) & -\kappa_1\mathrm{H}_0^{(2)}(\kappa_1\rho_1)
\end{vmatrix}, \tag{2.12}$$

and

$$g_1(\gamma^2, k) = \begin{vmatrix}
-\mathrm{J}_0(\kappa_0\rho_0) & \kappa_1\mathrm{H}_0^{(1)}(\kappa_1\rho_0) & \kappa_1\mathrm{H}_0^{(2)}(\kappa_1\rho_0)\\
-\dfrac{k\epsilon_0}{\kappa_0}\mathrm{J}_1(\kappa_0\rho_0) & k\epsilon_1\mathrm{H}_1^{(1)}(\kappa_1\rho_0) & k\epsilon_1\mathrm{H}_1^{(2)}(\kappa_1\rho_0)\\
0 & -k\epsilon_1\mathrm{H}_1^{(1)}(\kappa_1\rho_1) & -k\epsilon_1\mathrm{H}_1^{(2)}(\kappa_1\rho_1)
\end{vmatrix}. \tag{2.13}$$

By evaluating the determinants (2.12) and (2.13) above along its last row, it is found that

$$\begin{cases} f_1(\gamma^2,k) = -k\epsilon_1\kappa_1 a_1(\kappa_1) f_0(\gamma^2,k) - \kappa_1^2 b_1(\kappa_1) g_0(\gamma^2,k), \\ g_1(\gamma^2,k) = -k^2\epsilon_1^2 c_1(\kappa_1) f_0(\gamma^2,k) - k\epsilon_1\kappa_1 d_1(\kappa_1) g_0(\gamma^2,k), \end{cases} \tag{2.14}$$

where the definitions in (2.10) have been employed (for $i = 1$), as well as (2.11).

In order to formulate the general determinants, the following simplified notation is introduced

$$\begin{cases} x_{i,j}^{(1)} = \kappa_i \mathrm{H}_0^{(1)}(\kappa_i\rho_j) \\ y_{i,j}^{(1)} = k\epsilon_i \mathrm{H}_1^{(1)}(\kappa_i\rho_j) \end{cases}, \quad \begin{cases} x_{i,j}^{(2)} = \kappa_i \mathrm{H}_0^{(2)}(\kappa_i\rho_j) \\ y_{i,j}^{(2)} = k\epsilon_i \mathrm{H}_1^{(2)}(\kappa_i\rho_j) \end{cases}, \tag{2.15}$$

where $i \geq 1$ and $j = i-1, i$. The ith order determinants are now given by

$$f_i(\gamma^2,k) = \begin{vmatrix} f_0 & x_{1,0}^{(1)} & x_{1,0}^{(2)} & & \\ g_0 & y_{1,0}^{(1)} & y_{1,0}^{(2)} & & \\ & \ddots & \ddots & & \\ & -x_{i-1,i-1}^{(1)} & -x_{i-1,i-1}^{(2)} & x_{i,i-1}^{(1)} & x_{i,i-1}^{(2)} \\ & -y_{i-1,i-1}^{(1)} & -y_{i-1,i-1}^{(2)} & y_{i,i-1}^{(1)} & y_{i,i-1}^{(2)} \\ & & & -x_{i,i}^{(1)} & -x_{i,i}^{(2)} \end{vmatrix}, \tag{2.16}$$

and

$$g_i(\gamma^2,k) = \begin{vmatrix} f_0 & x_{1,0}^{(1)} & x_{1,0}^{(2)} & & \\ g_0 & y_{1,0}^{(1)} & y_{1,0}^{(2)} & & \\ & \ddots & \ddots & & \\ & -x_{i-1,i-1}^{(1)} & -x_{i-1,i-1}^{(2)} & x_{i,i-1}^{(1)} & x_{i,i-1}^{(2)} \\ & -y_{i-1,i-1}^{(1)} & -y_{i-1,i-1}^{(2)} & y_{i,i-1}^{(1)} & y_{i,i-1}^{(2)} \\ & & & -y_{i,i}^{(1)} & -y_{i,i}^{(2)} \end{vmatrix}, \tag{2.17}$$

where $i \geq 2$. By evaluating the determinants (2.16) and (2.17) above along its last row, the following layer-recursive relation is now obtained

$$\begin{cases} f_i = -k\epsilon_i\kappa_i a_i(\kappa_i) f_{i-1} - \kappa_i^2 b_i(\kappa_i) g_{i-1}, \\ g_i = -k^2\epsilon_i^2 c_i(\kappa_i) f_{i-1} - k\epsilon_i\kappa_i d_i(\kappa_i) g_{i-1}, \end{cases} \tag{2.18}$$

where the definitions in (2.10) have been employed as well as (2.16) and (2.17), and where the arguments (γ^2, k) have been suppresed for simplicity. Note that the recursive relation (2.18) is valid for $1 \leq i \leq N$.

The dispersion relation for a multi-layered coaxial cable where the last boundary at radius ρ_N is a Perfectly Electrically Conducting (PEC) surface, is given by

$$f_N(\gamma^2,k) = 0. \tag{2.19}$$

The corresponding condition $g_N(\gamma^2, k) = 0$ can be interpreted similarly as the dispersion relation associated with a Perfectly Magnetically Conducting (PMC) surface at radius ρ_N. Here, we are interested mainly in the dispersion relation including the exterior domain, as defined in (2.9) above. Hence, the complete determinant based on all of the boundary conditions in (2.6) through (2.8) can finally be expressed as

$$h_{N+1} = k\epsilon_{N+1}\mathrm{H}_1^{(2)}(\kappa_{N+1}\rho_N)f_N - \kappa_{N+1}\mathrm{H}_0^{(2)}(\kappa_{N+1}\rho_N)g_N, \tag{2.20}$$

where f_N and g_N can be computed recursively by using (2.11) and (2.18).

3 Asymptotic analysis

3.1 The Weierstrass preparation theorem

The following theorem by Weierstrass provides important insight into the derivation of the asymptotic behavior of the propagation constant, *cf.*, Theorem 7.5.1 in [6]. In particular, the theorem will be used to establish the low-frequency behavior of the two functions f_N and g_N defined in (2.18) above.

Theorem 3.1. (The Weierstrass preparation theorem)
Let $f(w, z)$ be an analytic function of $(w, z) \in \mathbb{C} \times \mathbb{C}$ in a neighborhood of $(0, 0)$ such that

$$\begin{cases} f = \dfrac{\partial f}{\partial w} = \ldots = \dfrac{\partial^{n-1} f}{\partial w^{n-1}} = 0, \\ \dfrac{\partial^n f}{\partial w^n} \neq 0, \end{cases} \tag{3.1}$$

at $(0, 0)$. Then there is a unique factorization

$$f(w, z) = a(w, z)\left(w^n + b_{n-1}(z)w^{n-1} + \ldots + b_0(z)\right), \tag{3.2}$$

where $b_j(z)$ and $a(w, z)$ are analytic in a neighborhood of 0 and $(0, 0)$, respectively, $a(0, 0) \neq 0$ and $b_j(0) = 0$.

In the present context, the Theorem 3.1 will be used as follows. Let $(w, z) = (\gamma^2, k)$ and suppose that $f(\gamma^2, k)$ is analytic in a neighborhood of $(0, 0)$. Suppose further that the following relations have been established

$$\begin{cases} f = 0, \\ \dfrac{\partial f}{\partial \gamma^2} \neq 0, \end{cases} \tag{3.3}$$

at $(\gamma^2, k) = (0, 0)$. It follows then from Theorem 3.1 that

$$f(\gamma^2, k) = a(\gamma^2, k)\left(\gamma^2 + b_0(k)\right), \tag{3.4}$$

where $a(0, 0) \neq 0$. Hence, a zero $\gamma^2(k)$ of f which is analytic in a neighborhood of $k = 0$, is uniquely given by

$$\gamma^2(k) = -b_0(k), \tag{3.5}$$

where $b_0(0) = 0$.

3.2 Basic asymptotics

To analyze the low-frequency asymptotic properties of (2.20), it is important to separate the logarithmic singularities of the Hankel functions in the definition of the auxiliary functions (2.10). The following definitions and asymptotic expansions for small arguments (as $z \to 0$) will be used throughout the analysis, see [12]. The Bessel functions of the first kind and order $m = 0, 1$ are given by

$$\mathrm{J}_0(z) = 1 - \frac{1}{4}z^2 + \mathcal{O}\{z^4\}, \tag{3.6}$$

$$\mathrm{J}_1(z) = \frac{1}{2}z + \mathcal{O}\{z^3\}, \tag{3.7}$$

where $\mathrm{J}_1(z) = -\mathrm{J}_0'(z)$, and where the big ordo notation $\mathcal{O}\{\cdot\}$ is defined as in [11, 12]. The Bessel function of the second kind and order $m = 0$ is given by

$$\mathrm{Y}_0(z) = \frac{2}{\pi}\left(\ln\frac{z}{2} + \tilde{\gamma}\right)\mathrm{J}_0(z) + A(z), \tag{3.8}$$

where $\tilde{\gamma}$ is Euler's constant and $A(z)$ the analytic function given by

$$A(z) = \frac{2}{\pi}\sum_{k=1}^{\infty}\frac{(-1)^{k+1}(z^2/4)^k}{(k!)^2}\sum_{l=1}^{k}\frac{1}{l} = \frac{1}{2\pi}z^2 + \mathcal{O}\{z^4\}. \tag{3.9}$$

The function $\mathrm{Y}_0(z)$ can hence also be expressed as

$$\mathrm{Y}_0(z) = \frac{2}{\pi}\ln\frac{z}{2}\mathrm{J}_0(z) + B(z), \tag{3.10}$$

where $B(z)$ is the analytic function

$$B(z) = \frac{2}{\pi}\tilde{\gamma}\mathrm{J}_0(z) + A(z) = \frac{2}{\pi}\tilde{\gamma} + \frac{1-\tilde{\gamma}}{2\pi}z^2 + \mathcal{O}\{z^4\}. \tag{3.11}$$

The Bessel function of the second kind and order $m = 1$ is given by

$$\mathrm{Y}_1(z) = \frac{2}{\pi}\ln\frac{z}{2}\mathrm{J}_1(z) + C(z), \tag{3.12}$$

where $\mathrm{Y}_1(z) = -\mathrm{Y}_0'(z)$ has been used, and where $C(z)$ is the meromorphic function

$$C(z) = -\frac{2}{\pi}\frac{1}{z}\mathrm{J}_0(z) - B'(z) = -\frac{2}{\pi}\frac{1}{z} + \frac{2\tilde{\gamma}-1}{2\pi}z + \mathcal{O}\{z^3\}. \tag{3.13}$$

The Hankel functions of the first and second kind are defined by $\mathrm{H}_m^{(1)}(z) = \mathrm{J}_m(z) + \mathrm{i}\mathrm{Y}_m(z)$ and $\mathrm{H}_m^{(2)}(z) = \mathrm{J}_m(z) - \mathrm{i}\mathrm{Y}_m(z)$, respectively. From the definitions (3.10) and (3.12) follows that

$$\mathrm{H}_0^{(1)}(z) = \mathrm{J}_0(z) + \mathrm{i}B(z) + \mathrm{i}\frac{2}{\pi}\ln\frac{z}{2}\mathrm{J}_0(z), \tag{3.14}$$

$$\mathrm{H}_0^{(2)}(z) = \mathrm{J}_0(z) - \mathrm{i}B(z) - \mathrm{i}\frac{2}{\pi}\ln\frac{z}{2}\mathrm{J}_0(z), \tag{3.15}$$

$$\mathrm{H}_1^{(1)}(z) = \mathrm{J}_1(z) + \mathrm{i}C(z) + \mathrm{i}\frac{2}{\pi}\ln\frac{z}{2}\mathrm{J}_1(z), \tag{3.16}$$

$$\mathrm{H}_1^{(2)}(z) = \mathrm{J}_1(z) - \mathrm{i}C(z) - \mathrm{i}\frac{2}{\pi}\ln\frac{z}{2}\mathrm{J}_1(z). \tag{3.17}$$

By inserting (3.14) through (3.17) into the expressions for the auxiliary functions defined in (2.10), it follows that

$$\begin{aligned} a_i(\kappa_i) = {} & \mathrm{i}\tfrac{4}{\pi}\mathrm{J}_0(\kappa_i\rho_i)\mathrm{J}_1(\kappa_i\rho_{i-1})\ln(\rho_{i-1}/\rho_i) \\ & -\mathrm{i}2B(\kappa_i\rho_i)\mathrm{J}_1(\kappa_i\rho_{i-1}) + \mathrm{i}2C(\kappa_i\rho_{i-1})\mathrm{J}_0(\kappa_i\rho_i), \end{aligned} \tag{3.18}$$

$$\begin{aligned} b_i(\kappa_i) = {} & \mathrm{i}\tfrac{4}{\pi}\mathrm{J}_0(\kappa_i\rho_{i-1})\mathrm{J}_0(\kappa_i\rho_i)\ln(\rho_i/\rho_{i-1}) \\ & +\mathrm{i}2B(\kappa_i\rho_i)\mathrm{J}_0(\kappa_i\rho_{i-1}) - \mathrm{i}2B(\kappa_i\rho_{i-1})\mathrm{J}_0(\kappa_i\rho_i), \end{aligned} \tag{3.19}$$

$$\begin{aligned} c_i(\kappa_i) = {} & \mathrm{i}\tfrac{4}{\pi}\mathrm{J}_1(\kappa_i\rho_{i-1})\mathrm{J}_1(\kappa_i\rho_i)\ln(\rho_{i-1}/\rho_i) \\ & -\mathrm{i}2C(\kappa_i\rho_i)\mathrm{J}_1(\kappa_i\rho_{i-1}) + \mathrm{i}2C(\kappa_i\rho_{i-1})\mathrm{J}_1(\kappa_i\rho_i), \end{aligned} \tag{3.20}$$

and

$$\begin{aligned} d_i(\kappa_i) = {} & \mathrm{i}\tfrac{4}{\pi}\mathrm{J}_0(\kappa_i\rho_{i-1})\mathrm{J}_1(\kappa_i\rho_i)\ln(\rho_i/\rho_{i-1}) \\ & -\mathrm{i}2B(\kappa_i\rho_{i-1})\mathrm{J}_1(\kappa_i\rho_i) + \mathrm{i}2C(\kappa_i\rho_i)\mathrm{J}_0(\kappa_i\rho_{i-1}). \end{aligned} \tag{3.21}$$

Note that the logarithmic singularities of the Hankel functions used in (2.10) vanish, and the auxiliary functions which are given by (3.18) through (3.21) are meromorphic in a neighborhood of $\kappa_i = 0$.

Based on (3.6), (3.7), (3.11) and (3.13), the following asymptotic expansions of the auxiliary functions defined in (2.10) can now be derived

$$a_i(\kappa_i) = \frac{1}{\kappa_i}\left(-\mathrm{i}\frac{4}{\pi}\frac{1}{\rho_{i-1}}\right) + \mathcal{O}\{\kappa_i\}, \tag{3.22}$$

$$b_i(\kappa_i) = \mathrm{i}\frac{4}{\pi}\ln\frac{\rho_i}{\rho_{i-1}} + \mathcal{O}\{\kappa_i^2\}, \tag{3.23}$$

$$c_i(\kappa_i) = \mathrm{i}\frac{2}{\pi}\left(\frac{\rho_{i-1}}{\rho_i} - \frac{\rho_i}{\rho_{i-1}}\right) + \mathcal{O}\{\kappa_i^2\}, \tag{3.24}$$

$$d_i(\kappa_i) = \frac{1}{\kappa_i}\left(-\mathrm{i}\frac{4}{\pi}\frac{1}{\rho_i}\right) + \mathcal{O}\{\kappa_i\}. \tag{3.25}$$

3.3 Asymptotic analysis for the subdeterminants

An asymptotic analysis based on Theorem 3.1 is given below regarding the subdeterminants $f_i(\gamma^2, k)$ and $g_i(\gamma^2, k)$ defined in (2.11) and (2.18) for all inner regions $i = 0, 1, \ldots, N$. Throughout the analysis, it will be assumed that there is one isolating layer with $\sigma_j = 0$ for $2 \leq j \leq N-1$. All other layers are conducting, semiconducting or poorly isolating with $\sigma_i \neq 0$ if $i \neq j$ and $i = 0, \ldots, N$.

The following frequency dependent parameters will be used based on (2.2) and (2.3)

$$k\epsilon_i = k\epsilon_{\mathrm{r}i} - \mathrm{i}\sigma_i\eta_0, \tag{3.26}$$

$$\kappa_i^2 = k^2\epsilon_{\mathrm{r}i} - \mathrm{i}\sigma_i\eta_0 k + \gamma^2, \tag{3.27}$$

and it is seen immediately that $\kappa_i = 0$ when $(\gamma^2, k) = (0, 0)$.

By observing that f_0 and g_0 defined in (2.11) are even analytic functions of κ_0, and that the functions $\kappa_i a_i(\kappa_i)$, $b_i(\kappa_i)$, $c_i(\kappa_i)$ and $\kappa_i d_i(\kappa_i)$ given by (3.22) through (3.25) are all even analytic functions of κ_i (and hence analytic functions of κ_i^2), it is concluded that the functions f_i and g_i defined recursively in (2.18), are all analytic functions in a neighborhood of $(\gamma^2, k) = (0, 0)$ for $i = 1, \ldots, N$. The values of f_i and g_i at $(\gamma^2, k) = (0, 0)$ are denoted $f_i(0)$ and $g_i(0)$, respectively.

Based on (3.22) through (3.25), the following asymptotic expressions are now obtained for (2.11) and (2.18)

$$f_0 = -1 + \mathcal{O}\{\kappa_0^2\}, \tag{3.28}$$

$$g_0 = -\left(k\epsilon_{\mathrm{r}0} - \mathrm{i}\sigma_0\eta_0\right)\left(\frac{1}{2}\rho_0 + \mathcal{O}\{\kappa_0^2\}\right), \tag{3.29}$$

and

$$\begin{aligned} f_i &= -\left(k\epsilon_{\mathrm{r}i} - \mathrm{i}\sigma_i\eta_0\right)\left(-\frac{\mathrm{i}4}{\pi}\frac{1}{\rho_{i-1}} + \mathcal{O}\{\kappa_i^2\}\right) f_{i-1} \\ &\quad -\left(\kappa_i^2\frac{\mathrm{i}4}{\pi}\ln\frac{\rho_i}{\rho_{i-1}} + \mathcal{O}\{\kappa_i^4\}\right) g_{i-1}, \end{aligned} \tag{3.30}$$

$$\begin{aligned} g_i &= -\left(k\epsilon_{\mathrm{r}i} - \mathrm{i}\sigma_i\eta_0\right)^2\left(\frac{\mathrm{i}2}{\pi}\left(\frac{\rho_{i-1}}{\rho_i} - \frac{\rho_i}{\rho_{i-1}}\right) + \mathcal{O}\{\kappa_i^2\}\right) f_{i-1} \\ &\quad -\left(k\epsilon_{\mathrm{r}i} - \mathrm{i}\sigma_i\eta_0\right)\left(-\frac{\mathrm{i}4}{\pi}\frac{1}{\rho_i} + \mathcal{O}\{\kappa_i^2\}\right) g_{i-1}, \end{aligned} \tag{3.31}$$

where $1 \leq i \leq N$.

From (3.28) and (3.29) follows that

$$f_0(0) = -1, \tag{3.32}$$

$$g_0(0) = \mathrm{i}\sigma_0\eta_0\frac{1}{2}\rho_0, \tag{3.33}$$

and from (3.30) and (3.31)

$$f_i(0) = \sigma_i\eta_0\frac{4}{\pi}\frac{1}{\rho_{i-1}}f_{i-1}(0), \tag{3.34}$$

$$g_i(0) = \mathrm{i}\sigma_i^2\eta_0^2\frac{2}{\pi}\left(\frac{\rho_{i-1}}{\rho_i} - \frac{\rho_i}{\rho_{i-1}}\right) f_{i-1}(0) + \sigma_i\eta_0\frac{4}{\pi}\frac{1}{\rho_i}g_{i-1}(0), \tag{3.35}$$

where $1 \leq i \leq j-1$. By using the recursion above it can be shown that $f_i(0)$ is real with $f_i(0) < 0$ and $g_i(0)$ is imaginary with $\mathrm{Im}\{g_i(0)\} > 0$ for $i = 0, 1, \ldots, j-1$.

Since $\sigma_j = 0$, it follows directly from (3.30) and (3.31) that $f_i(0) = 0$ and $g_i(0) = 0$ for $i \geq j$. In particular, it is now concluded that $f_N(\gamma^2, k)$ is an analytic function in a neighborhood of $(0, 0)$, and that

$$f_N = 0, \tag{3.36}$$

at $(\gamma^2, k) = (0, 0)$.

The derivatives of f_i with respect to γ^2 are studied next. From (3.27) and (3.30) follows that

$$\frac{\partial f_j}{\partial \gamma^2} = \sum_{i=0}^{j} \frac{\partial f_j}{\partial \kappa_i^2} = -\mathrm{i}\frac{4}{\pi} \ln \frac{\rho_j}{\rho_{j-1}} g_{j-1}(0) \neq 0, \tag{3.37}$$

evaluated at $(\gamma^2, k) = (0, 0)$. Further, by employing that $f_i(0) = 0$ and $g_i(0) = 0$ for $i \geq j$, it follows also from (3.30) that

$$\frac{\partial f_i}{\partial \gamma^2} = \sigma_i \eta_0 \frac{4}{\pi} \frac{1}{\rho_{i-1}} \frac{\partial f_{i-1}}{\partial \gamma^2} \neq 0, \tag{3.38}$$

where $j + 1 \leq i \leq N$. Hence, it is finally concluded that

$$\frac{\partial f_N}{\partial \gamma^2} \neq 0, \tag{3.39}$$

at $(\gamma^2, k) = (0, 0)$, and the prerequisites of the Weierstrass preparation theorem are fulfilled as stated in (3.3). It follows now from Theorem 3.1 that f_N can be uniquely factorized as

$$f_N(\gamma^2, k) = a(\gamma^2, k) \left(\gamma^2 + b_0(k)\right), \tag{3.40}$$

where $a(0, 0) \neq 0$ and $b_0(k)$ is an analytic function where $b_0(0) = 0$.

The implication of the factorization in (3.40) is that the function f_N has a unique zero $\gamma^2(k) = -b_0(k)$ which is an analytic function in a neighborhood of $k = 0$, and where $\gamma^2(k) \to 0$ as $k \to 0$. To find the exact asymptotic behavior of the zero $\gamma^2(k)$, the following expansion is used

$$\gamma^2(k) = \mathrm{i}A^2 k + \mathcal{O}\{k^2\}, \tag{3.41}$$

which is based on a Taylor series expansion of $\gamma^2(k)$ where $\gamma^2(0) = 0$, and where even coefficients are real and odd coefficients are imaginary. Here, A is the real (or imaginary) constant to be determined. The low-frequency asymptotics of the radial wave numbers under the assumption (3.41) are given by

$$\kappa_i^2 = k^2 \epsilon_{\mathrm{r}i} - \mathrm{i}\sigma_i \eta_0 k + \gamma^2(k) = \mathrm{i}(A^2 - \sigma_i \eta_0) k + \mathcal{O}\{k^2\}. \tag{3.42}$$

The low-frequency asymptotics of the recursive relations (3.28) and (3.29), and (3.30) and (3.31) become

$$f_0 = -1 + \mathcal{O}\{k\}, \tag{3.43}$$

$$g_0 = -\left(k\epsilon_{\mathrm{r}0} - \mathrm{i}\sigma_0 \eta_0\right) \left(\frac{1}{2}\rho_0 + \mathcal{O}\{k\}\right), \tag{3.44}$$

and

$$\begin{aligned} f_i = {} & -\left(k\epsilon_{\mathrm{r}i} - \mathrm{i}\sigma_i \eta_0\right) \left(-\frac{\mathrm{i}4}{\pi} \frac{1}{\rho_{i-1}} + \mathcal{O}\{k\}\right) f_{i-1} \\ & - \left(\left(\mathrm{i}(A^2 - \sigma_i \eta_0) k + \mathcal{O}\{k^2\}\right) \frac{\mathrm{i}4}{\pi} \ln \frac{\rho_i}{\rho_{i-1}} + \mathcal{O}\{k^2\}\right) g_{i-1}, \end{aligned} \tag{3.45}$$

$$\begin{aligned} g_i = {} & -\left(k\epsilon_{\mathrm{r}i} - \mathrm{i}\sigma_i \eta_0\right)^2 \left(\frac{\mathrm{i}2}{\pi} \left(\frac{\rho_{i-1}}{\rho_i} - \frac{\rho_i}{\rho_{i-1}}\right) + \mathcal{O}\{k\}\right) f_{i-1} \\ & - \left(k\epsilon_{\mathrm{r}i} - \mathrm{i}\sigma_i \eta_0\right) \left(-\frac{\mathrm{i}4}{\pi} \frac{1}{\rho_i} + \mathcal{O}\{k\}\right) g_{i-1}, \end{aligned} \tag{3.46}$$

where $1 \leq i \leq N$.

Let $f_i(k) = f_i(\gamma^2(k), k)$ and $g_i(k) = g_i(\gamma^2(k), k)$. Since $\sigma_j = 0$ for one isolating layer j with $2 \leq j \leq N-1$ and $\sigma_i \neq 0$ if $i \neq j$ and $i = 0, \ldots, N$, it follows from (3.43) through (3.46) above that

$$\begin{cases} f_i(k) = \mathcal{O}\{1\} & 0 \leq i \leq j-1, \\ g_i(k) = \mathcal{O}\{1\} & 0 \leq i \leq j-1, \end{cases} \tag{3.47}$$

and

$$\begin{cases} f_i(k) = \mathcal{O}\{k\} & j \leq i \leq N, \\ g_i(k) = \mathcal{O}\{k\} & j \leq i \leq N. \end{cases} \tag{3.48}$$

In particular, the first order term of $f_j(k)$ is given by

$$[k^{-1} f_j(k)]_0 = \mathrm{i}\epsilon_{\mathrm{r}j} \frac{4}{\pi} \frac{1}{\rho_{j-1}} f_{j-1}(0) + A^2 \frac{4}{\pi} \ln \frac{\rho_j}{\rho_{j-1}} g_{j-1}(0), \tag{3.49}$$

where $f_{j-1}(0)$ and $g_{j-1}(0)$ are given recursively by (3.34) and (3.35). The first order term of $f_i(k)$ for $j+1 \leq i \leq N$ (where $\sigma_i \neq 0$) is given by

$$[k^{-1} f_i(k)]_0 = \sigma_i \eta_0 \frac{4}{\pi} \frac{1}{\rho_{i-1}} [k^{-1} f_{i-1}(k)]_0, \tag{3.50}$$

and hence finally

$$[k^{-1} f_N(k)]_0 = \frac{\sigma_{j+1} \cdots \sigma_N}{\rho_j \cdots \rho_{N-1}} \left(\eta_0 \frac{4}{\pi} \right)^{N-j} [k^{-1} f_j(k)]_0. \tag{3.51}$$

Since $\gamma^2(k)$ is assumed to be a zero of f_N, it is concluded that the term $[k^{-1} f_N(k)]_0$ as well as the term $[k^{-1} f_j(k)]_0$ vanishes, and hence from (3.49)

$$A^2 = \frac{-\mathrm{i}\epsilon_{\mathrm{r}j} f_{j-1}(0)}{\rho_{j-1} \ln \frac{\rho_j}{\rho_{j-1}} g_{j-1}(0)}, \tag{3.52}$$

where $f_{j-1}(0)$ and $g_{j-1}(0)$ are given by (3.34) and (3.35). It is observed that A^2 is a real and positive constant. Finally, the low frequency asymptotics of the propagation constant $\gamma(k)$ corresponding to the dispersion relation $f_N = 0$, is given by

$$\gamma(k) = A\sqrt{\mathrm{i}k} + \mathcal{O}\{k\sqrt{k}\}, \tag{3.53}$$

where A is the positive square root of (3.52).

3.4 Asymptotic analysis of the dispersion relation

The dispersion relation $h_{N+1} = 0$ defined by (2.20) will finally be analyzed below. As before, it will be assumed that there is one isolating layer with $\sigma_j = 0$ for $2 \leq j \leq N-1$. All other layers are conducting, semiconducting or poorly isolating with $\sigma_i \neq 0$ if $i \neq j$ and $i = 0, \ldots, N+1$.

A dispersion function which is bounded in a neighborhood of $(\gamma^2, k) = (0, 0)$ is defined as follows

$$\begin{aligned} h(\gamma^2, k) &= \kappa_{N+1} h_{N+1}(\gamma^2, k) \\ &= k\epsilon_{N+1}\kappa_{N+1}\mathrm{H}_1^{(2)}(\kappa_{N+1}\rho_N) f_N - \kappa_{N+1}^2 \mathrm{H}_0^{(2)}(\kappa_{N+1}\rho_N) g_N. \end{aligned} \tag{3.54}$$

Based on the definitions (3.15) and (3.17) and the asymptotics (3.6), (3.7), (3.11) and (3.13), it is concluded that

$$\kappa_{N+1}\mathrm{H}_1^{(2)}(\kappa_{N+1}\rho_N) = \mathrm{i}\frac{2}{\pi}\frac{1}{\rho_N} + \mathcal{O}\{\kappa_{N+1}\}, \tag{3.55}$$

$$\kappa_{N+1}^2\mathrm{H}_0^{(2)}(\kappa_{N+1}\rho_N) = \mathcal{O}\{\kappa_{N+1}\}, \tag{3.56}$$

where the following property of the logarithm has been used

$$\mathcal{O}\{z^n\} \ln z = \mathcal{O}\{z^{n-1}\}, \tag{3.57}$$

where $n \geq 1$. The dispersion function (3.54) can therefore be written as

$$h(\gamma^2, k) = (k\epsilon_{\mathrm{r}(N+1)} - \mathrm{i}\sigma_{N+1}\eta_0)\left(\mathrm{i}\frac{2}{\pi}\frac{1}{\rho_N} + \mathcal{O}\{\kappa_{N+1}\}\right) f_N + \mathcal{O}\{\kappa_{N+1}\} g_N. \tag{3.58}$$

It is noted that $h = 0$ at $(\gamma^2, k) = (0, 0)$, but the branch-cut of the logarithm remains and h is not a continuous function in a neighborhood of $(\gamma^2, k) = (0, 0)$.

It will be shown below that there exists a solution to the dispersion relation $h = 0$, which can be uniquely expressed as

$$\gamma^2(k) = \mathrm{i}A^2 k + o\{k\}, \tag{3.59}$$

or equivalently $\gamma(k) = A\sqrt{\mathrm{i}k} + o\{\sqrt{k}\}$, where A^2 is given by (3.52) and where the little ordo notation $o\{\cdot\}$ is defined as in *e.g.*, [11, 12]. The solution (3.59) is unique in the sense that there is no other solution $\gamma^2(k)$ which converges faster towards zero, as $k \to 0$.

To prove (3.59), it is first assumed that

$$\gamma^2(k) = ck + o\{k\}, \tag{3.60}$$

where c is a constant. The transversal wave numbers are then given by

$$\kappa_i^2 = k^2\epsilon_{\mathrm{r}i} - \mathrm{i}\sigma_i\eta_0 k + \gamma^2(k) = \mathcal{O}\{k\}. \tag{3.61}$$

The low-frequency asymptotics of the recursive relations (3.28) and (3.29), and (3.30) and (3.31) become

$$f_0 = -1 + \mathcal{O}\{k\}, \tag{3.62}$$

$$g_0 = -(k\epsilon_{\mathrm{r}0} - \mathrm{i}\sigma_0\eta_0)\left(\frac{1}{2}\rho_0 + \mathcal{O}\{k\}\right), \tag{3.63}$$

and

$$f_i = -\left(k\epsilon_{\mathrm{r}i} - \mathrm{i}\sigma_i\eta_0\right)\left(-\frac{\mathrm{i}4}{\pi}\frac{1}{\rho_{i-1}} + \mathcal{O}\{k\}\right) f_{i-1} + \mathcal{O}\{k\}g_{i-1}, \tag{3.64}$$

$$\begin{aligned} g_i = & -\left(k\epsilon_{\mathrm{r}i} - \mathrm{i}\sigma_i\eta_0\right)^2\left(\frac{\mathrm{i}2}{\pi}\left(\frac{\rho_{i-1}}{\rho_i} - \frac{\rho_i}{\rho_{i-1}}\right) + \mathcal{O}\{k\}\right) f_{i-1} \\ & -\left(k\epsilon_{\mathrm{r}i} - \mathrm{i}\sigma_i\eta_0\right)\left(-\frac{\mathrm{i}4}{\pi}\frac{1}{\rho_i} + \mathcal{O}\{k\}\right) g_{i-1}, \end{aligned} \tag{3.65}$$

where $1 \leq i \leq N$.

As before, let $f_i(k) = f_i(\gamma^2(k), k)$ and $g_i(k) = g_i(\gamma^2(k), k)$. Since $\sigma_j = 0$ and $\sigma_i \neq 0$ for $i \neq j$, it follows from (3.62) through (3.65) above that

$$\begin{cases} f_i(k) = \mathcal{O}\{1\} & 0 \leq i \leq j-1, \\ g_i(k) = \mathcal{O}\{1\} & 0 \leq i \leq j-1, \end{cases} \tag{3.66}$$

and

$$\begin{cases} f_i(k) = \mathcal{O}\{k\} & j \leq i \leq N, \\ g_i(k) = \mathcal{O}\{k\} & j \leq i \leq N. \end{cases} \tag{3.67}$$

The dispersion function (3.58) becomes

$$\begin{aligned} h(\gamma^2, k) = & \left(k\epsilon_{\mathrm{r}(N+1)} - \mathrm{i}\sigma_{N+1}\eta_0\right)\left(\mathrm{i}\frac{2}{\pi}\frac{1}{\rho_N} + \mathcal{O}\{k^{1/2}\}\right) \\ & a(\gamma^2(k), k)\left(\gamma^2 - \mathrm{i}A^2k + \mathcal{O}\{k^2\}\right) + \mathcal{O}\{k^{1/2}\}\mathcal{O}\{k\}, \end{aligned} \tag{3.68}$$

where the factorization (3.40) based on Weierstrass preparation theorem has been used and where $a(0,0) \neq 0$, $b_0(k) = -\mathrm{i}A^2k + \mathcal{O}\{k^2\}$ and A^2 is given by (3.52).

To establish the existence of the solution (3.59), it is assumed that $\gamma^2 = \mathrm{i}A^2k + r\mathrm{e}^{\mathrm{i}\theta}k$ where r is an arbitrary positive constant and $\theta \in [0, 2\pi]$. The dispersion function (3.68) becomes

$$h(\gamma^2, k) = k\left(\sigma_{N+1}\eta_0\frac{2}{\pi}\frac{1}{\rho_N}a(0,0)r\mathrm{e}^{\mathrm{i}\theta} + \mathcal{O}\{k^{1/2}\}\right). \tag{3.69}$$

Note that the wave numbers $\kappa_i = \sqrt{k^2\epsilon_{\mathrm{r}i} - \mathrm{i}\sigma_i\eta_0 k + \mathrm{i}A^2k + r\mathrm{e}^{\mathrm{i}\theta}k}$ converges to zero uniformly over θ, as $k \to 0$. From the asymptotic analysis above, it can therefore be concluded that the expression $\mathcal{O}\{k^{1/2}\}$ in (3.69) also converges uniformly to zero, as $k \to 0$. Hence, it follows from (3.69) that if k is sufficiently small, then the argument variation of h is $\Delta \arg h = 2\pi$ for $\theta \in [0, 2\pi]$, and there exists a single zero of h within the circle defined by $\gamma^2 = \mathrm{i}A^2k + r\mathrm{e}^{\mathrm{i}\theta}k$. This zero can now be written in the form of (3.60).

To establish the uniqueness of the solution (3.59), it is assumed that $\gamma^2(k) = ck + o\{k\}$ where c is a constant. The dispersion relation based on (3.68) can then be written to its lowest order as

$$\sigma_{N+1}\eta_0\frac{2}{\pi}\frac{1}{\rho_N}a(0,0)\left(c - \mathrm{i}A^2\right)k + o\{k\} = 0, \tag{3.70}$$

which shows that $c = \mathrm{i}A^2$. It is noted that the asymptotic expressions (3.68) and (3.70) which are based on the assumption (3.60), are valid also when $c = 0$. Hence, the assumption that $c = 0$ leads to a contradiction. In conclusion, there can be no zeros of h of the form $\gamma^2(k) = o\{k\}$, and (3.59) expresses the unique solution which has the fastest convergence towards zero, as $k \to 0$.

4 Numerical examples

The low-frequency asymptotic behavior derived in (3.59) is compared below with the result of a numerical method. The numerical computation of the propagation constant has been described in [10]. The numerical solution is stable at low frequencies, and numerical problems due to the ill-conditioning of the boundary conditions arise only at higher frequencies. As an example problem is considered the low-frequency dispersion behavior of the TM_{01} mode of an extruded HVDC sea cable as depicted in Figure 2 below.

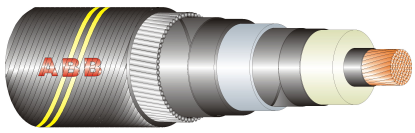

Figure 2: Cross-section of an extruded HVDC sea cable.

The geometrical and electrical parameters of the model is given by Table 1 below. Here, the permittivity of the insulation, the semi-conducting XLPE screens, the inner sheat and the outer serving are modeled with $\epsilon_{\mathrm{d}} = 2.3$. The conductivity of the semi-conducting XLPE screens [13, 16] are modeled with $\sigma_{\mathrm{s}} = 1\,\mathrm{S/m}$. The conductivity of the inner conductor, the lead sheat and the armour are modeled with $\sigma_{\mathrm{Cu}} = 5.8 \cdot 10^7\,\mathrm{S/m}$, $\sigma_{\mathrm{Pb}} = 4.6 \cdot 10^6\,\mathrm{S/m}$ and $\sigma_{\mathrm{Fe}} = 1.1 \cdot 10^6\,\mathrm{S/m}$, respectively. The conductivity of the isolating sheets for $i = 5$ and $i = 7$ are modeled either with $\sigma_{\mathrm{is}} = 0$ or $\sigma_{\mathrm{is}} = 10^{-12}\,\mathrm{S/m}$. Note that the insulating layer is considered to be a perfect insulator with $\sigma_2 = 0$. Hence, $\sigma_j = 0$ with $j = 2$ according to the notation adopted previously in this paper. The conductivity of the exterior region is modeled either with $\sigma_{\mathrm{ext}} = 0$ or $\sigma_{\mathrm{ext}} = 0.1\,\mathrm{S/m}$.

The numerical method has been validated using experimental data based on time domain measurements as described in [10]. In Figure 3 is shown similarly a comparison between measurements and modeling regarding the transmission of a pulse along an 82 km long HVDC power cable that was rolled up on shore. These results were obtained by numerical computation of the propagation constant and the characteristic impedance of the cable at 8192 frequency points in the frequency interval $0 - 100\,\mathrm{kHz}$, taking into account the mismatch between the measurement devices and the power cable, and finally by performing an Inverse Fast Fourier Transformation (IFFT), see [10].

In Figures 4 and 5 are shown the wave propagation characteristics of the modeled cable over the low-frequency range $0 - 1000\,\mathrm{Hz}$. Here, the conductivity of the

Layer	radius [mm]	permittivity	conductivity
Inner conductor	$\rho_0 = 24.3$	$\epsilon_{r0} = 1$	$\sigma_0 = \sigma_{Cu}$
Conductor screen	$\rho_1 = 26.0$	$\epsilon_{r1} = \epsilon_d$	$\sigma_1 = \sigma_s$
Insulation	$\rho_2 = 42.0$	$\epsilon_{r2} = \epsilon_d$	$\sigma_2 = 0$
Insulation screen	$\rho_3 = 43.9$	$\epsilon_{r3} = \epsilon_d$	$\sigma_3 = \sigma_s$
Lead sheat	$\rho_4 = 46.9$	$\epsilon_{r4} = 1$	$\sigma_4 = \sigma_{Pb}$
Inner sheat	$\rho_5 = 49.5$	$\epsilon_{r5} = \epsilon_d$	$\sigma_5 = \sigma_{is}$
Armour	$\rho_6 = 53.5$	$\epsilon_{r6} = 1$	$\sigma_6 = \sigma_{Fe}$
Outer serving	$\rho_7 = 58.5$	$\epsilon_{r7} = \epsilon_d$	$\sigma_7 = \sigma_{is}$
Exterior region	$\rho_8 = \infty$	$\epsilon_{r8} = 1$	$\sigma_8 = \sigma_{ext}$

Table 1: Modeling parameters.

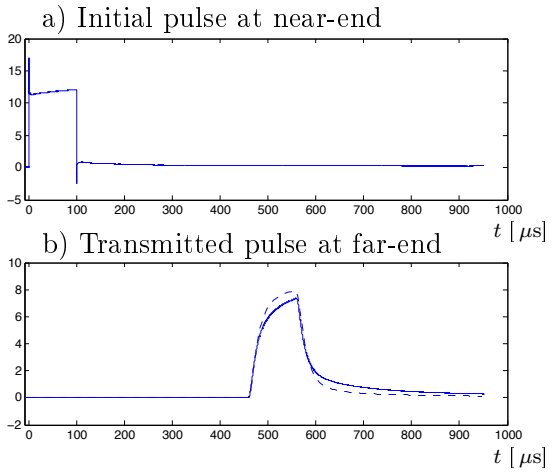

Figure 3: Comparison between measurements and modeling. In a) is shown the initial pulse at the near-end and in b) the transmitted pulse at the far-end. The solid lines show the measured pulses and in b) the dashed line shows the modeled pulse. The conductivity of the isolating sheets ($i = 5, 7$) is $\sigma_{is} = 0$ and the exterior conductivity is $\sigma_{ext} = 0$.

isolating sheets ($i = 5, 7$) is $\sigma_{is} = 0$. The plots illustrate that the significance of the exterior conductivity σ_{ext} is minor, and is noticeable only at the lower frequencies below 200-300 Hz.

In Figure 6 is shown the computed low-frequency behavior of the propagation constant together with the dominating term $A\sqrt{ik}$ of the low-frequency asymptotics given by (3.59).

In Figure 7 is illustrated the low-frequency asymptotics of the propagation constant as $k \to 0$. In this plot, the propagation constant has been normalized with $\bar{\gamma} = \gamma/\mathrm{Re}\{\gamma_0\}$ where γ_0 is the asymptotic solution $\gamma_0 = A\sqrt{ik}$. According to the asymptotic expression (3.59), $\bar{\gamma}$ should approach $1+\mathrm{i}$ as $k \to 0$. This is in agreement with the behavior of the numerical solution as illustrated in Figure 7.

In this example case regarding the HVDC power cable, it is concluded that the

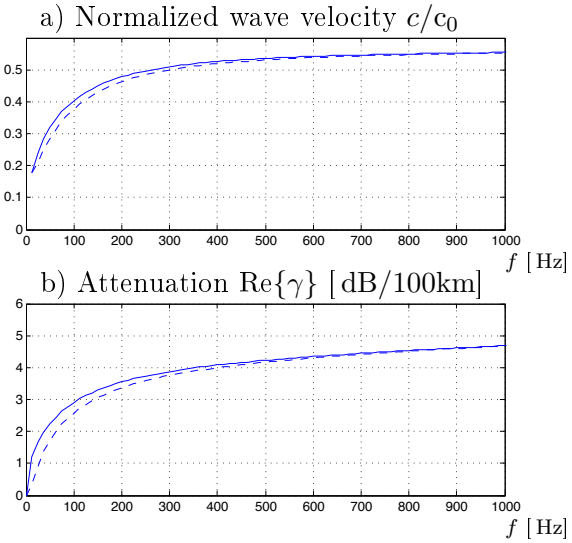

Figure 4: Low-frequency dispersion characteristics for the coaxial cable: a) Normalized wave velocity $c/c_0 = k/\mathrm{Im}\{\gamma(k)\}$. b) Attenuation $2 \cdot 10^6 \log \mathrm{e} \cdot \mathrm{Re}\{\gamma\}$ in dB/100km. The solid lines show the modeled dispersion characteristics with exterior conductivity $\sigma_{\mathrm{ext}} = 0$ and the dashed lines with $\sigma_{\mathrm{ext}} = 0.1\,\mathrm{S/m}$.

first order asymptotic expansion $\gamma \sim A\sqrt{\mathrm{i}k}$ is accurate only for frequencies well below 1 Hz, and is hence not accurate enough to model time domain pulses which are measured over the relevant frequency range of about $0 - 100\,\mathrm{kHz}$. An accurate numerical solution to the dispersion relation is therefore very useful, see also [10].

5 Summary and conclusions

An exact asymptotic analysis regarding the low-frequency dispersion characteristics of the multi-layered coaxial cable has been given in this paper. A layer-recursive description of the dispersion relation has been derived and analyzed. It has been shown that if there is one isolating layer and a perfectly conducting outer shield, the classical Weierstrass preparation theorem can be used to prove that the low-frequency behavior of the propagation constant is governed by a square root of the complex frequency, and an exact analytical expression for the dominating term of the asymptotic expansion has been derived. It has furthermore been shown that the same asymptotic expansion is valid to its lowest order even if the outer shield has finite conductivity and there is an infinite exterior region with finite non-zero conductivity. The proofs have been conducted on the basis of asymptotic analysis, and illustrated with numerical examples.

As a practical application of the theory, a High-Voltage Direct Current (HVDC) power cable has been analyzed and a numerical solution to the dispersion relation has been validated by comparisons with the asymptotic analysis. The comparison reveals that the low-frequency characteristics of the power cable is very complicated

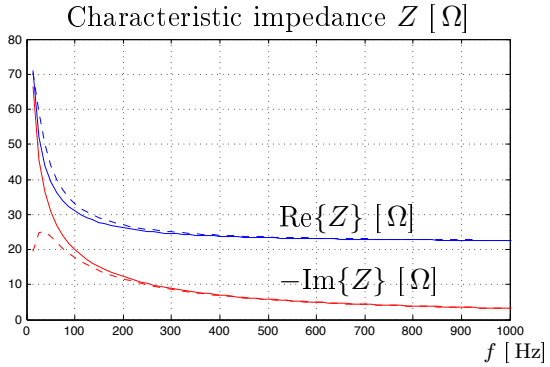

Figure 5: Low-frequency impedance characteristics for the coaxial cable. The blue lines show $\mathrm{Re}\{Z\}$ and the red lines show $-\mathrm{Im}\{Z\}$. The solid lines show the modeled impedance characteristics with exterior conductivity $\sigma_{\mathrm{ext}} = 0$ and the dashed lines with $\sigma_{\mathrm{ext}} = 0.1\,\mathrm{S/m}$.

and a first order asymptotic approximation is valid only at the lowest frequencies below 1 Hz. Hence, for practical modeling purposes such as with fault localization or cable length estimation, an accurate numerical solution to the dispersion relation is of great value.

Acknowledgements

This work was supported in part by the Swedish Research Council (VR) and ABB AB. The authors are also grateful to ABB AB for providing the opportunity to perform the cable measurements on their premises.

References

[1] N. Amekawa, N. Nagaoka, and Y. Baba. Derivation of a semiconducting layer impedance and its effect on wave propagation characteristics on a cable. *IEE Proceedings – Generation, Transmission & Distribution*, **150**(4), 434–441, 2003.

[2] S. Boggs, A. Pathak, and P. Walker. Partial discharge. XXII. High frequency attenuation in shielded solid dielectric power cable and implications thereof for PD location. *IEEE Electrical Insulation Magazine*, **12**(1), 9–16, 1996.

[3] A. Boström, G. Kristensson, and S. Ström. Transformation properties of plane, spherical and cylindrical scalar and vector wave functions. In V. V. Varadan, A. Lakhtakia, and V. K. Varadan, editors, *Field Representations and Introduction to Scattering*, Acoustic, Electromagnetic and Elastic Wave Scattering, chapter 4, pages 165–210. Elsevier Science Publishers, Amsterdam, 1991.

[4] J. R. Carson and J. J. Gilbert. Transmission characteristic of the submarine cable. *Journal of the Franklin Institute*, **192**(6), 705–735, 1921.

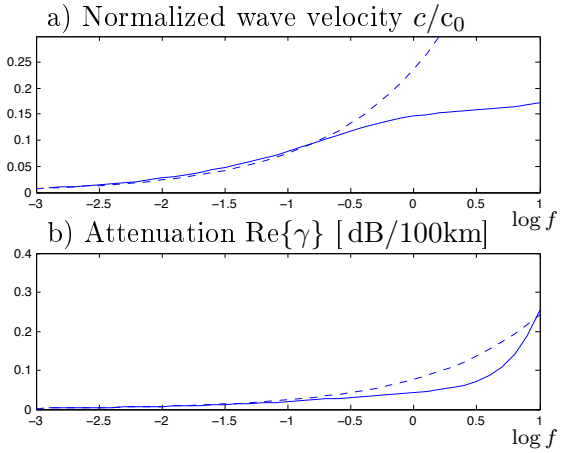

Figure 6: Low-frequency asymptotics of the dispersion characteristics for the coaxial cable: a) Normalized wave velocity $c/c_0 = k/\mathrm{Im}\{\gamma(k)\}$. b) Attenuation $2 \cdot 10^6 \log \mathrm{e} \mathrm{Re}\{\gamma\}$ in dB/100km. The solid line shows the numerical solution and the dashed line shows the low-frequency asymptotics based on the expression $\gamma \sim A\sqrt{\mathrm{i}k}$ where $k = 2\pi f/c_0$. The conductivity of the isolating sheets ($i = 5, 7$) are $\sigma_{\mathrm{is}} = 10^{-12}\,\mathrm{S/m}$ and the exterior conductivity is $\sigma_{\mathrm{ext}} = 0.1\,\mathrm{S/m}$.

[5] F. E. Gardiol. *Lossy transmission lines.* Artech House, Boston, London, 1987.

[6] L. Hörmander. *The Analysis of Linear Partial Differential Operators I.* Grundlehren der mathematischen Wissenschaften 256. Springer-Verlag, Berlin Heidelberg, 1983.

[7] J. D. Jackson. *Classical Electrodynamics.* John Wiley & Sons, New York, third edition, 1999.

[8] J. Lundbäck, S. Nordebo, and T. Biro. A digital directional coupler with applications to partial discharge measurements. *IEEE Transactions on Instrumentation and Measurements*, **57**(11), 2561–2567, 2008.

[9] J. Lundstedt. Condition for distortionfree transmission lines with a nonuniform characteristic impedance. *IEEE Trans. Microwave Theory Tech.*, **43**(6), 1386–1389, 1995.

[10] S. Nordebo, B. Nilsson, T. Biro, G. Cinar, M. Gustafsson, S. Gustafsson, A. Karlsson, and M. Sjöberg. Electromagnetic dispersion modeling and measurements for HVDC power cables. Technical Report LUTEDX/(TEAT-7211)/1–32/(2011), Lund University, Department of Electrical and Information Technology, P.O. Box 118, S-221 00 Lund, Sweden, 2011. http://www.eit.lth.se.

[11] F. W. J. Olver. *Asymptotics and special functions.* A K Peters, Ltd, Natick, Massachusetts, 1997.

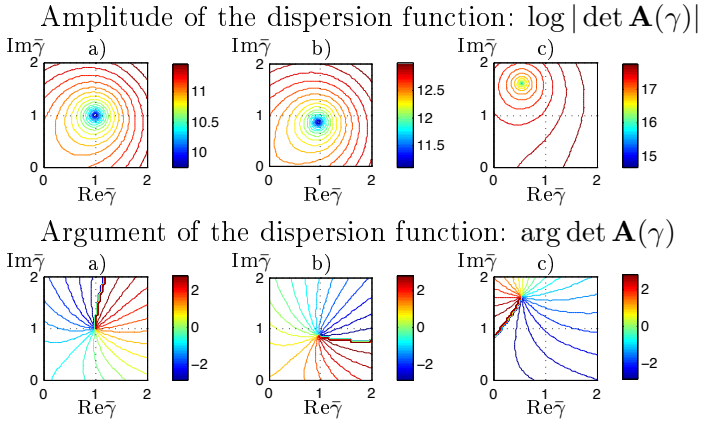

Figure 7: Illustration of the low-frequency asymptotics of the propagation constant $\gamma(k)$ where $k = 2\pi f/\mathrm{c}_0$. The upper and lower plots show the amplitude and the argument of the dispersion function $\det \mathbf{A}(\gamma)$, respectively, for a) $f = 10^{-4}\,\mathrm{Hz}$, b) $f = 10^{-2}\,\mathrm{Hz}$ and c) $f = 1\,\mathrm{Hz}$. The axes are normalized with $\bar{\gamma} = \gamma/\mathrm{Re}\{\gamma_0\}$ where γ_0 is the asymptotic solution $\gamma_0 = A\sqrt{ik}$. The conductivity of the isolating sheets $(i = 5, 7)$ is $\sigma_{\mathrm{is}} = 10^{-12}\,\mathrm{S/m}$ and the exterior conductivity is $\sigma_{\mathrm{ext}} = 0.1\,\mathrm{S/m}$.

[12] F. W. J. Olver, D. W. Lozier, R. F. Boisvert, and C. W. Clark. *NIST Handbook of mathematical functions*. Cambridge University Press, New York, 2010.

[13] R. Papazyan, P. Pettersson, and D. Pommerenke. Wave propagation on power cables with special regard to metallic screen design. *IEEE Transactions on Dielectrics and Electrical Insulation*, **14**(2), 409–416, 2007.

[14] D. Pommerenke, T. Strehl, R. Heinrich, W. Kalkner, F. Schmidt, and W. Weissenberg. Discrimination between interal PD and other pulses using directional coupling sensors on HV cable systems. *IEEE Transactions on Dielectrics and Electrical Insulation*, **6**(6), 814–824, Dec. 1999.

[15] D. M. Pozar. *Microwave Engineering*. John Wiley & Sons, New York, third edition, 2005.

[16] K. Steinbrich. Influence of semiconducting layers on the attenuation behaviour of single-core power cables. *IEE Proceedings - Generation, Transmission and Distribution*, **152**(2), 271–276, 2005.

[17] G. C. Stone. Partial discharge diagnostics and electrical equipment insulation condition assessment. *IEEE Transactions on Dielectrics and Electrical Insulation*, **12**(5), 891–905, 2005.

[18] C.-T. Tai. Dyadic Green's functions for a coaxial line. *IEEE Trans. Antennas Propagat.*, **31**(2), 355–358, 1983.

[19] J. Veen. *On-line signal analysis of partial discharges in medium-voltage power cables*. Phd thesis, Eindhoven University of Technology, the Netherlands, 2005.